$[\{Fe(PEt_3)_3\}_2(\mu\text{-}H)_6B][BPh_4]$: A Complex Containing Octahedral Hypercoordinate Boron

Anna C. Hillier, Heiko Jacobsen, Dimitri Gusev, Helmut W. Schmalle, and Heinz Berke*

Anorganisch-Chemisches Institut, Universität Zürich,-Winterthurerstrasse 190, CH-8057 Zürich, Switzerland

Received May 7, 2001

Introduction

A hypervalent[1] molecule is described as one in which the octet rule is not obeyed in the sense that there are more than four pairs of electrons in the conventional Lewis diagram for the molecule.[2] The bonding in such molecules involves formal expansion of the valence shell. Hypervalent compounds of the first-row elements boron,[3] carbon,[4] and fluorine[5] have been reported. During our work on metal hydrides, we have isolated an unusual iron hydride complex which appears to fall into this category.[6]

Results and Discussion

The reaction of $FeCl_2$ with PEt_3 and $NaBH_4$ in ethanol affords dinuclear "$[\{Fe(PEt_3)_3\}_2(BH_6)]^+$", isolated as its BPh_4 salt (**1**). Venanzi has previously reported the related $[\{RuH(CH_3C(CH_2PPh_2)_3)\}_2(BH_4)]^+$ (**2**).[7] The temperature-invariant (183−323 K) ^1H and ^{31}P NMR spectra of **1** display only one hydride and one phosphine environment. The broad hydride signal for **1** is at rather high field for a B−H−M bridging hydrogen (δ −14.25 ppm), compared to δ −4.90 ppm for **2**, although similar shifts have been noted elsewhere.[8] On decoupling from ^{31}P, the hydride signal sharpens, surprisingly since coupling between bridging hydrogens and phosphine ^{31}P nuclei is rarely observed in transition metal borohydride complexes. No such sharpening is observed in the $^1H\{^{11}B\}$ NMR spectrum. The broad Fe−*B*−Fe signal at δ 60 ppm ($\nu_{1/2}$ = 800 Hz) in the ^{11}B NMR spectrum is at the low-field end of the tridentate BX_3 range,[9] close to shifts observed for boron atoms with direct metal−boron bonds.[10] Owing to the unexpected NMR spectral data, a crystal structure determination of **1** was undertaken.

Orange prisms of **1** were grown by slow diffusion of pentane into a concentrated THF solution of **1** at −40 °C. Crystallographic data are given in Table 1. The study revealed a discrete dinuclear $[\{Fe(PEt_3)_3\}_2(\mu\text{-}H)_6B]^+$ cation with a separated $[BPh_4]^-$ counterion. The structure of the cation is shown in Figure 1 with the atomic numbering scheme and selected bond distances. All the Fe−H bond distances are essentially the same, as are the Fe−P distances, giving distorted octahedral environments at each Fe atom. The P−Fe−Fe−P dihedral angles lie between 40° and 80°, i.e., the FeP_3H_3 units are effectively staggered, but twisted 20° from the ideal geometry. The B(1)−H distances are comparable, suggesting an octahedral environment for the boron atom, but longer than expected from known structural data on bridging hydrogens in borohydride complexes (generally 100−140 pm). The Fe−B distances are close to the sum of the covalent radii of Fe and B (205 pm),[11] corroborating the Fe−B−Fe bonding interaction suggested by the ^{11}B NMR spectrum. The structure of **1** differs, therefore, from that reported for **2**, where notably the Ru−P(*trans*-H) bond is longer than those trans to the bridging BH_4^- hydrogens and the P−Ru−Ru−P dihedral angles vary from 1° to 110°. Short Ru−B distances were, however, also reported. Our X-ray study suggests, therefore, that the best description of the cation in **1** is $[\{Fe(PEt_3)_3\}_2(\mu\text{-}H)_6B]^+$.

In order to assist in the characterization of the unusual coordination geometry of **1**, we carried out density functional calculations[12] on the two model compounds $[\{Fe(PH_3)_3(H)_3\}_2B]^+$ **I** and $[\{FeH(PH_3)_3\}_2(BH_4)]^+$ **II**. Although modeling real phosphine ligands by the prototypical PH_3 molecule might sometimes have implications on the relative energies of possible isomers,[13] molecular geometries are generally well represented by the model systems, and one should also be able to establish the characteristic bonding features around the boron center. Optimized structures for the model compounds are displayed in Figure 2. Both of these structures represent local minima on the potential hypersurface of virtually the same energy, and our calculations therefore suggest that both coordination geometries might be viable alternatives for compound **1** and related species. In **I**, we have six identical hydrogen ligands with almost equal Fe−H and B−H bond distances around 155 pm, indicating D_{3d} local symmetry at boron, whereas in **II**, we find two single Fe−H bonds, and four bridging hydrogens with distinctly different *d*(Fe−H) and *d*(B−H) separations. The latter, at 136

(1) (a) Musher, J. I. *Angew. Chem., Int. Ed. Engl*. **1969**, *8*, 54. (b) Akiba, K.-Y. *Chemistry of Hypervalent Compounds*; Wiley-VCH: New York, 1999.
(2) Gillespie, R. J.; Robinson, E. A. *Inorg. Chem*. **1995**, *34*, 978 and references therein.
(3) Lee, D. Y.; Martin, J. C. *J. Am. Chem. Soc*. **1984**, *106*, 5745.
(4) (a) Akiba, K.-y.; Yamashita, M.; Yamamoto, Y.; Nagase, S. *J. Am. Chem. Soc*. **1999**, *121*, 10644. (b) G. Plah, A.; White, A. M.; O'Brien, D. H. *Chem. Rev*. **1979**, *70*, 561. (c) Olah, G. A.; Rasul, G. *Acc. Chem. Res*. **1997**, *30*, 245. (d) Schleyer, P. v. R.; Würthwein, E.-U.; Kaufmann, E.; Clark, T.; Pople, J. A. *J. Am. Chem. Soc*. **1983**, *105*, 5930. (e) Kudo, H. *Nature* **1992**, *355*, 432. (f) Scherbaum, F.; Grohmann, A.; Müller, G.; Schmidbaur, H. *Angew. Chem., Int. Ed. Engl*. **1989**, *28*, 463.
(5) Ault, B. S.; Andrews, L. *Inorg. Chem*. **1977**, *16*, 2024.
(6) Gusev, D. G.; Hübener, R.; Burger, P.; Orama, O.; Berke, H. *J. Am. Chem. Soc*. **1997**, *119*, 3716.
(7) Rhodes, L. F.; Venanzi, L. M.; Sorato, C.; Albinati, A. *Inorg. Chem*. **1986**, *25*, 3337.
(8) (a) Ghilardi, C. A.; Innocenti, P.; Midollini, S.; Orlandini, A. *J. Chem. Soc., Dalton Trans*. **1985**, 605. (b) Jacobsen, G. B.; Andersen, E. L.; Housecroft, C. E.; Hong, F.-E.; Buhl, M. L.; Long, G. J.; Fehlner, T. P. *Inorg. Chem*. **1987**, *26*, 4040.
(9) Kennedy, J. D. In *Multinuclear NMR*; Mason, J., Ed.; Plenum Press: New York, 1987.
(10) (a) Rath, N. P.; Fehlner, T. P. *J. Am. Chem. Soc*. **1988**, *110*, 5345, (b) Fehlner, T. P.; Czech, P. T.; Fenske, R. F. *Inorg. Chem*. **1990**, *29*, 3103.
(11) Emsley, J. *The Elements*, 2nd ed.; Oxford University Press: Oxford, 1991.
(12) The BP86 calculations (Becke, A. D. *Phys. Rev*. **1988**, *A38*, 3098; Perdew, J. P. *Phys. Rev*. **1986**, *B33*, 8822) utilized the program system TURBOMOLE (Ahlrichs, R.; Bär, M.; Häser, M.; Horn, H.; Kölmel, C. *Chem. Phys. Lett*. **1989**, *162*, 165; Treutler, O.; Ahlrichs, R. *J. Chem. Phys*. **1995** *102*, 346; Eichkorn, K.; Treutler, O.; Öhm, H.; Häser, M.; Ahlrichs, R. *Chem. Phys. Lett*. **1995**, *242*, 652; Eichkorn, K.; Weigend, F.; Treutler, O.; Ahlrichs, R. *Theor. Chem. Acc*. **1997**, *97*, 119). A triple-ζ valence basis plus polarization (TZVP) was employed (Schäfer, A.; Huber, C.; Ahlrichs, R. *J. Chem. Phys*. **1994**, *100*, 5829), except for the H atoms of the phosphine groups, which were treated with a split valence plus polarization basis set (SVP) (Schäfer, A.; Horn, H.; Ahlrichs, R. *J. Chem. Phys*. **1992**, *97*, 2571). Optimized geometries and calculated frequencies are to be found in the Supporting Information section.
(13) Jacobsen, H.; Berke H. *Chem. Eur. J*. **1997**, *3*, 881.

10.1021/ic010477r CCC: $20.00
Published on Web 10/20/2001

Table 1. Experimental Data for the X-ray Study of Compound **1**

empirical formula	$C_{60}H_{116}B_2P_6Fe_2$
fw	1156.67
temp, K	183(2)
wavelength, Å	0.71073
space group	$P\bar{1}$
unit cell dimens	
a, Å	11.7396(8)
b, Å	15.9566(11)
c, Å	17.8324(12)
α, deg	77.947(8)
β, deg	83.942(8)
γ, deg	89.176(8)
V, Å^3	3248.5(4)
Z	2
ρ_{calcd}, mg m^{-3}	1.183
μ(Mo Kα), cm^{-1}	6.29
final *R* indices [$I > 2\sigma(I)$]	R1 = 0.0472, wR2 = 0.1026

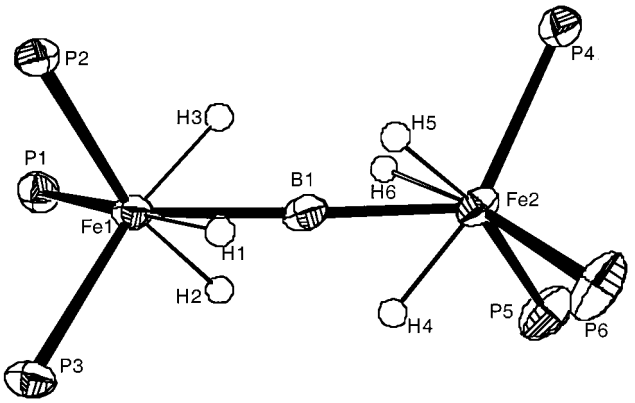

Figure 1. ORTEP view of cation **1**. Carbon and non-hydride hydrogen atoms are omitted for clarity. Relevant bond lengths (in pm): Fe(1)−B(1) 190.3(3); Fe(2)−B(1) 191.3(3); Fe(1)−P(1) 223.67(8); Fe(1)−P(2) 221.92(6); Fe(1)−P(3) 222.64(6); Fe(2)−P(4) 223.28(7); Fe(2)−P(5) 224.62(7); Fe(2)−P(6) 223.74(8); Fe(1)−H(1) 154(2); Fe(1)−H(2) 154.7(18); Fe(1)−H(3) 150.0(19); Fe(2)−H(4) 152.3(19); Fe(2)−H(5) 153.0(19); Fe(2)−H(6) 154(2); B(1)−H(1) 148.2(19); B(1)−H(2) 155.8(19); B(1)−H(3) 153(2); B(1)−H(4) 149.2(19); B(1)−H(5) 159-(2); B(1)−H(6) 150.1(19).

pm, are well within the usual range of B−H distances of μ-H ligands in tetrahydroborate complexes. The Fe−B bond is somewhat longer in **II**, and the Fe−P bond trans to the hydride ligand is elongated by 4 pm, compared to the other phosphine groups. These observations, together with the closer match of the P−M−M−P torsion angles in **1** with those for **I** than for **II**, indicate a pseudo-octahedral arrangement of hydrogens around boron in **1**. A recent theoretical study suggests that the BH_6^+ cation should be viewed as containing two dihydrogen units, i.e., as $[B(H)_2(H_2)_2]^+$ rather than as an octahedral unit.[14] The difference in our case presumably arises from the presence of the $Fe(PEt_3)_3$ moieties and the strong Fe−H interaction.

The question remains as to how the chemical bonding around the boron center might be characterized. In **II**, the main structural motif is a $[BH_4]^-$ anion bridging two metal moieties. The structure and bonding of transition metal tetrahydroborato complexes has recently been reviewed,[15] and we refer the reader to the literature for a detailed description of the orbital interactions of a $[BH_4]^-$ unit bridging two metal centers. Of more interest is the D_{3d} geometry **I**, which appears to be an example for a hypervalent boron center. However, a caveat is in order. While the term *hypervalence* still is one of the main bonding concepts taught in inorganic chemistry curricula,[16] it

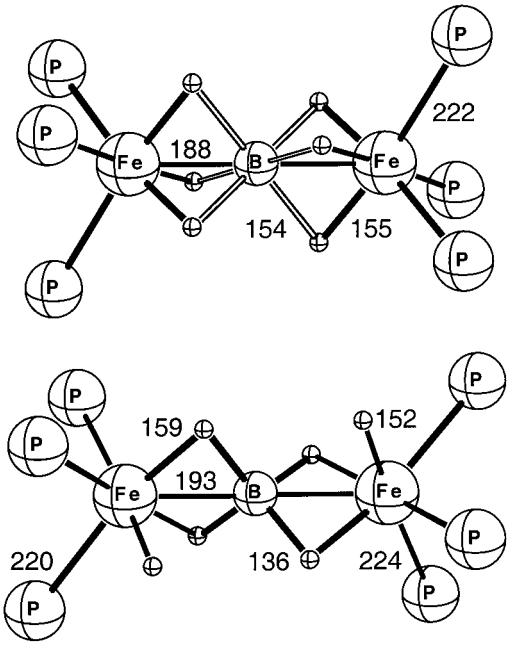

Figure 2. Optimized BP86 geometries and selected bond distances (in pm) for the $[\{Fe(PH_3)(H)_3\}_2B]^+$ model compounds **I** (above) and **II** (below) (P = PH_3).

becomes more and more clear that this is an unnecessary concept,[2] which mystifies rather than clarifies the bonding situation. Thus, it would be better to talk about *hypercoordination* instead, in particular when considering that an orbital analysis of so-called hypervalent compounds leads to the conclusion that the octet rule per se is not violated.[17] For structure **I**, a partial orbital diagram is presented in Figure 3, which also contains sketches[18] of those molecular orbitals responsible for Fe−H and B−H bonding. The degenerate $1e_u$ set is made up of Fe−H bonding orbitals on each of the metal centers, which interact with boron-based p_x and p_y orbitals, respectively. The nature of the metal fragment orbitals can clearly be seen in the corresponding $1e_g$ orbital, which for symmetry reasons does not bear any boron contributions. The combination $2e_u$, which is B−H bonding, but Fe−H antibonding, constitutes the LUMO of **I**, which underlines the fact that the occupied orbital $1e_u$ to a major extent contributes to Fe−H bonding interaction. The orbital $1a_{2u}$ is dominated by d_{z^2} and p_z functions at iron, as well as p_z at boron, and thus constitutes Fe−B bonding. The next orbital, $2a_{2u}$, which does not carry any contribution from boron, again is Fe−H bonding in character. From this orbital analysis one might draw the conclusion that system **I** should be described as two anionic $[(PH_3)_3FeH_3]^-$ units linked by a B^{3+} center, and that the Fe−B bond is supported by secondary B−H interactions. A topological analysis[19] of the electron density $\rho(\mathbf{r})$ supports this description. In particular, gradient paths of the gradient vector field $\nabla\rho(\mathbf{r})$, which originate at a bond critical point and terminate at the nuclei, might be used to define a chemical bond, and to establish a molecular graph. Such a graph for the bridging region of **I** is

(14) Jursic, B. S. *J. Mol. Struct. (THEOCHEM)* **1999**, *492*, 97.
(15) Xu, Z. T.; Lin, Z. Y. *Coord. Chem. Rev.* **1996**, *156*, 139.
(16) See, for example: Shriver, D. F.; Atkins, P. W.; Langford, C. H. *Inorganic Chemsitry*, 2nd ed.; Oxford University Press: Oxford, 1994.
(17) Albright, T. A.; Burdett, J. K.; Whangboo, M.-H. *Orbital Interactions in Chemistry*; John Wiley: New York, 1985; Chapter 14.
(18) The orbital pictures were generated with the help of the program Molden (Schaftenaar, G.; Noordik, J. H. *J. Comput.-Aided Mol. Des.* **2000**, *14*, 123.)
(19) (a) Bader, R. W. F. *Atoms in molecules. A quantum theory;* Clarendon Press: Oxford, 1990. (b) Popelier, P. L. A. *Atoms in molecules. An introduction*; Pearson Education: Harlow, 1999.

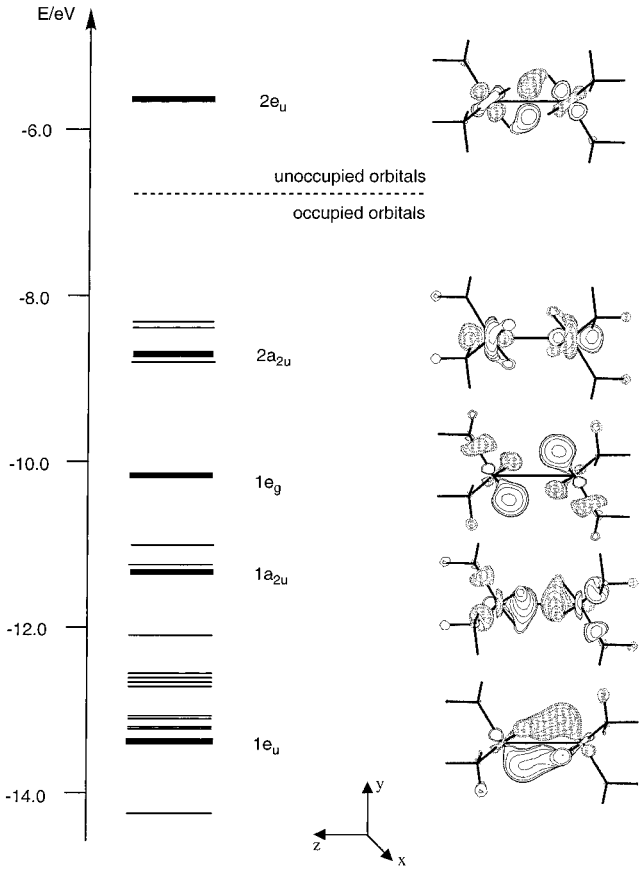

Figure 3. Orbital energy levels for **I**, labeled according to D_{3d} symmetry. Selected orbitals are also depicted, for which the corresponding energy lines appear in bold.

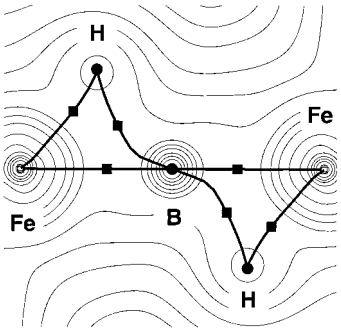

Figure 4. Contour lines of the charge density (thin) and the molecular graph (bold) in the bridging region of **I**. Bond critical points are denoted by squares (■).

shown[20] in Figure 4. We see bond paths, which connect the μ-H ligands with the iron as well as the boron centers. The curvature of the B−H path indicates that this bond is different from a typical covalent linkage. This conclusion is corroborated by an inspection of the bond ellipticities ϵ,[21] which not only characterize the extent to which charge is preferentially accumulated but also provide a measure for structural stability.[22] The calculated ϵ values for the Fe−B, Fe−H, and B−H bonds amount to 0.01, 0.65, and 1.39 au and point to a structural instability of the B−H bond. The topological analysis reveals certain similarities between the agostic M−H bond as found for transition metal complexes,[23] and the B−H bond in **I**.

Conclusions

Our calculations point to the fact that the prevailing structural motif in **1** is the pseudo-octahedral environment at the central boron. This is in accord with the outcome of the X-ray structure determination. The lowering of the symmetry from O_h to D_{3d} is presumably responsible for the broad ^{11}B NMR signal. A topological analysis has revealed the nature of the weak B−H bonding interactions which stabilize the structure by establishing a pseudo-octahedral surrounding of H ligands at boron. This unusual hypercoordination of a boron atom by hydrides is unprecedented, making **1** an unusual example of a boron analogue of the so-called hypervalent second-period main group species.

Experimental Section

General Procedures and Measurements. All operations were carried out under nitrogen atmosphere using standard Schlenk line and glovebox techniques. Solvents were distilled from Na/Ph_2CO (THF, pentane) (THF was predried over KOH). Absolute ethanol and methanol over molecular sieves were purchased from Fluka and degassed by bubbling dry dinitrogen through the solvent in a syringe immediately prior to injection. C_4D_8O used in NMR experiments was predried over sodium, then dried, and stored over sodium/potassium alloy (3:1 Na/K). The following reagents were purchased from commercial suppliers and used as received: $FeCl_2$ (anhydrous), Na[BPh_4] (Fluka), $NaBH_4$ (Aldrich), PEt_3 (Alfa). ^{1}H, ^{13}C, ^{31}P, and ^{11}B NMR experiments were carried out on a Varian Gemini-300 (operating at 300.1, 75.4, 121.5, and 96.2 MHz, respectively), or a Bruker DRX500 spectrometer (operating at 500.2, 125.8, 202.5, and 160.5 MHz, respectively). ^{1}H and ^{13}C{^{1}H} NMR spectra were referenced to the residual proton or ^{13}C resonances of the deuterated solvent. ^{31}P chemical shifts were externally referenced to 85% H_3PO_4 and ^{11}B chemical shifts to BF_3/OEt_2. IR spectra were recorded on a BIO RAD FTS-45 spectrophotometer as KBr pellets. Raman measurements were made on a Renishaw Ramascope instrument, on samples sealed under nitrogen in capillary tubes.

Synthesis of [{Fe(PEt_3)$_3$}$_2$(μ-H)$_6$B][BPh_4] (1). To a solution of $FeCl_2$ (0.40 g, 3.16 mmol) in ethanol (20 mL) was added PEt_3 (1.3 mL, 9.47 mmol); then the mixture was stirred for 20 min and cooled to −50 °C, and $NaBH_4$ (0.18 g, 4.75 mmol) was added. The deep red mixture was stirred for 6 h while warming to room temperature, during which time it turned orange/brown. After filtration, solvent was removed from the filtrate in vacuo and the yellow product washed with hexane (3 × 20 mL) and then dried under dynamic vacuum. The product was dissolved in methanol (15 mL), and then $NaBPh_4$ (0.53 g, 1.58 mmol) was added to form a yellow precipitate. After stirring for 15 min, the precipitate was allowed to settle and the solvent decanted off. The precipitate was washed with a further 2 × 20 mL of methanol, then dried, dissolved in THF, filtered over Celite, and dried in vacuo to afford 0.25 g (0.22 mmol, 14%) of **1**. Elemental microanal. Calcd for $C_{60}H_{116}P_6B_2Fe_2$: C, 62.30; H, 10.11. Found: C, 62.32; H, 10.31. IR (KBr pellet, cm^{-1}): 1884 (s, br) ν_{BH}/ν_{FeH}. Raman (solid, cm^{-1}): 1931 (m, br) ν_{BH}/ν_{FeH}. ^{1}H NMR (300 MHz, [D_8]THF, 293 K): δ 7.26 (br s, 8 H, BPh_4); 6.83 (t, 8 H, BPh_4); 6.68 (t, 4 H, BPh_4); 1.67 (m, 36 H, P(CH_2CH_3)$_3$); 1.12 (m, 54 H, P(CH_2CH_3)$_3$); −14.25 (br, 6 H, Fe−*H*). ^{31}P NMR (121.47 MHz, [D_8]THF, 293 K): δ 49.53 (s, *P*Et_3). ^{13}C NMR (75.47 MHz, [D_8]THF, 293 K): δ 137.56 (s, BPh_4); 125.91 (s, BPh_4); 122.01 (s, BPh_4); 24.26 (m, PCH_2CH_3); 8.87 (s, PCH_2CH_3). ^{11}B NMR (160.49 MHz, [D_8]THF, 293 K): δ 60 (br, Fe−*B*−Fe); −6.81 (s, *B*Ph_4).

X-ray Structure Analysis for 1. Crystal data and experimental details are listed in Table 1. Orange crystals were obtained by slow

(20) The topological analysis was performed using the program MORPHY (Popelier, P. L. A. *Comput. Phys. Commun.* **1996**, *92*, 212).

(21) Bond ellipticities ϵ are defined by the two principal curvatures λ_1 and λ_2 of $\rho(\mathbf{r})$ at the bond critical point: $\epsilon = (\lambda_2/\lambda_1) - 1$.

(22) Cremer, D.; Kraka, E.; Slee, T. S.; Bader, R. F. W.; Lau, C. D. H.; Nguyen-Dang, T. T.; MacDougall, P. J. *J. Am. Chem. Soc.* **1983**, *105*, 5069.

(23) (a) Popelier, P. L. A.; Logothetis, G. *J. Organomet. Chem.* **1998**, *555*, 101. (b) Scherer, W.; Hieringer, W.; Spiegler, M.; Sirsch, P.; McGrady, S.; Downs, A. J.; Haaland, A.; Pedersen, B. *Chem. Commun.* **1998**, 2471.

diffusion of pentane into a THF solution of **1** at −40 °C. A crystal (dimensions 0.47 × 0.37 × 0.33 mm) covered with hydrocarbon oil was mounted on top of a glass fiber and immediately transferred to the goniometer of a Stoe IPDS diffractometer, where it was cooled to 183(2) K using an Oxford Cryo System; 45324 reflection intensities were measured with graphite-monochromated Mo Kα radiation (λ = 0.71073 Å). ϕ-rotation scan, 1.1° rotations per image, total ϕ-rotation set to 240°, resulted in 218 images. Data were corrected for Lorentz and polarization effects and for absorption (numerical, 20 indexed crystal faces, transmission 0.8193−0.7565). The structure was solved with 17714 unique data (R_{int} = 0.0451) with direct methods using SHELXS-97.[24] The structure was refined by full-matrix least-squares methods on F^2 (wR2 = 0.1128) for all unique data and 655 parameters, R1 = 0.0472 for 10591 data with $I \geq 2\sigma(I)$, R1 for 17714 data was 0.0870. Three disordered ethyl groups were refined with partitioned positions with PART instruction of SHELXL-97. The six hydride atoms were located by difference electron density calculations. Their positions and isotropic displacement parameters were refined using soft restraint distances which were obtained from DFT calculations. All other positions of H atoms were calculated after each refinement cycle (riding model). The final maximum and minimum residual electron densities were 1.292 and −0.888 Å^{-3}.

(24) Sheldrick, G. M. SHELX-97: Software package for crystal structure determination: Universität Göttingen: Göttingen, Germany, 1997.

Acknowledgment. This work was supported by the University of Zürich and the Swiss National Science Foundation. We thank Dr. Thomas Fox for the NMR decoupling experiments. We also thank our referees for valuable suggestions.

Supporting Information Available: Optimized geometries and vibrational spectral data for **I** and **II**. This material is available free of charge via the Internet at http://pubs.acs.org. X-ray data: CCDC No. 151848.

IC010477R